Desalination and Water Treatment
www.deswater.com
doi: 10.1080/19443994.2014.958108

56 (2015) 1768–1775
November

Taylor & Francis
Taylor & Francis Group

Electrospun membranes of nanoporous structure cellulose acetate and its adsorptive behaviors using Copper(II) as models

Rui-Lai Liu[a,b], Chun-Yi Tang[c], Jin-Yun Zhao[b], Hai-Qing Liu[a,*]

[a]*College of Material Science and Engineering, Fujian Normal University, Fuzhou 350007, China, Tel./Fax: +86 599 5133136; emails: ruilailiu@163.com (R.-L. Liu), wyulrl@163.com (H.-Q. Liu)*
[b]*College of Ecological and Resource Engineering, Wuyi University, Wuyishan 354300, China*
[c]*College of Biological and Chemical Engineering, Guangxi University of Science and Technology, Liuzhou 545006, China*

Received 13 May 2014; Accepted 12 August 2014

ABSTRACT

Ribbon-like porous cellulose acetate (CA) ultrafine fibers with diameter of 0.94 ± 0.36 μm and pore size of 52×98 nm were prepared by electrospinning. The adsorption properties of Cu^{2+} on porous CA ultrafine fibers were studied. The maximum removal efficiencies of Cu^{2+} on CA membrane (MCA), CA ultrafine fibers (FCA), and porous CA ultrafine fibers (PFCA) were 19.1, 70.8, and 88.6%, respectively. This was attributed to the formation of nanoporous structure on the fibers surfaces, which increased the special surface area from 4.33 to 56.57 m^2/g. The adsorption data followed the Langmuir and Freundlich models. But the Langmuir model had better correlation at different temperatures. Based on the thermodynamic parameters, including ΔG°, ΔH°, and ΔS° calculated, the negative values of ΔG° indicated that the adsorption of Cu^{2+} on PFCA was spontaneous and thermodynamically favorable. The positive values of ΔH° demonstrate that the adsorption process belonged to endothermic nature, and revealed that high temperature is more beneficial for adsorption than low temperature. The positive value of ΔS° indicated that the randomness at the solid/solution interface with some structural changes in both the adsorbates and adsorbents during the adsorption process increased.

Keywords: Nanoporous; Cellulose acetate; Adsorption; Copper(II) ion

1. Introduction

Water pollution due to toxic heavy metals, such as cadmium, chromium, cobalt, copper, nickel, and mercury caused by industries and agricultural sources is one of the most serious environmental and public problems [1–3]. The contamination of water caused by heavy metals is a serious environmental problem due to their toxicity, persistency, and bioaccumulation tendency in nature. Therefore, it is necessary to take effective strategies to remove heavy metal ions from different effluents.

Various methods are available for removing heavy metals from aqueous solutions, including reverse osmosis [4], chemical precipitation [5], chemical oxidation/reduction [6], membrane separation processes [7], and ion-exchange [8]. Furthermore, some of these methods generate secondary pollutants, the disposal of which is an additional burden on the techno-economic feasibility of treatment procedures. These constraints have caused researchers to search for a

*Corresponding author.

simple, relatively low-cost, and effective method of removing heavy metals from wastewater. Adsorption is generally preferred for heavy metal ion removal due to its availability of different adsorbents, high efficiency, easily handling, reversibility, and possible low-cost. The main requirement for adsorbents is a low-cost/benefit ratio.

Electrospinning is a simple and versatile method for fabricating continuous fibers with diameters ranging from micrometers to several nanometers. The simplicity of the fabrication scheme, the diversity of materials suitable for use with electrospinning, as well as the unique and interesting features associated with electrospun nanofibers, all make this technique and resultant structures attractive for a number of applications, such as reinforced materials [9,10], photocatalysis [11,12], sensor [13,14], adsorbent [15,16] and filter materials [17,18], and so on.

Cellulose acetate (CA) is one of the most important plant-derived polymers because of its wide variety of applications [19]. Although chemically simple, cellulose is a structurally complex polymer, and several enzymes are required for the complete degradation of this molecule [20]. Moreover, CA can be usually used to treat wastewater as polymer materials. For example, native cellulose fibers were surface modified by poly (*N*,*N*-dimethyl aminoethyl methacrylate) (PDMAEMA) to generate an anion adsorbent, which had high efficiency in removal of F^-, AsO_2^-, and AsO_4^- from aqueous solutions, even at low initial concentrations. Tian et al. [21] had prepared cellulose acetate nanofibers membrane with a diameter of 0.5–1.5 μm by electrospinning and surface modification with poly(methacrylic acid) (PMAA). The adsorption of heavy metal ions Cu^{2+}, Hg^{2+}, and Cd^{2+} on this membrane was investigated. However, nanoporous structure cellulose acetate prepared by electrospinning for the adsorption of copper(II) ion had been rarely reported.

In this work, nanoporous structure CA fibers membranes were fabricated by electrospinning. The adsorption behaviors of nanoporous CA fibers membranes were evaluated by measuring the adsorption of Cu^{2+}. Subsequently, the adsorption equilibrium was simulated using the Langmuir and Freundlich isotherm models. The thermodynamic parameters were also well calculated and discussed in the system.

2. Experimental

2.1. Materials

N,*N*-dimethylformamide (DMF) and Dichloromethane (DCM) were purchased from Sinopharm Chemical Reagents Co., China. Then 1,000 mg L^{-1} of Copper(II) standard solution (Sinopharm Chemical Regent Co., China) was diluted by distilled water into work solutions described in the following experiments. Cellulose acetate (CA) with degree of substitution (DS) of 2.45 and an M_w of 3.0×10^4 was obtained from Sigma-Aldrich. All other chemicals were used as received.

2.2. Preparation of nanoporous CA fibrous membranes

CA spinning solutions of 12 wt.% were prepared by adding 0.5 g CA into 1:4 (v/v) acetone/DCM solvent mixtures, followed by magnetic stirring at ambient temperature. Spinning solution of 10 mL was immediately loaded into a plastic syringe equipped with 18-gauge stainless steel needle. The feeding rate was 20 μL/min monitored by a syringe pump (TS2-60, Longer Precision Pump Co. Ltd, Baoding, China). An electrode was clamped on the spinneret (stainless steel needle) and connected to a power supply (DW-P303-IAC, Tianjin Dongwen High Voltage Plant, China). A grounded counter electrode was connected to a collector aluminum foil, which was placed 10 cm away from the orifice. The applied voltage was kept at 10 kV. Nanoporous structure CA fibrous membranes on the grounded collector were collected, and then dried in a vacuum oven at 50°C for 5 h. Nanoporous structure CA fibrous membranes were coded as NPCA.

In comparison to NPCA, the non-porous CA fibrous membranes were prepared as follows: 12 wt.% CA-spinning solutions were prepared by adding 0.5 g CA into 1:2 (v/v) DMF/acetone solvent mixture. The non-porous CA fibrous membranes (coded as FCA) were fabricated by electrospinning (the method described above). The CA membranes (coded as MCA) were fabricated by casting method using 12 wt% CA solutions dissolved in 1:2 (v/v) DMF/acetone.

2.3. Adsorption experiments

5.0 mg L^{-1} Cu^{2+} was prepared by directly dissolving $CuSO_4$ in deionized water. The pH of the solutions was 4.0, adjusted by dilute NaOH and HCl aqueous solutions. The adsorption experiments were carried out by suspending 100 mg of PFCA, MCA, and FCA, respectively, in 50 mL solution of 5.0 mg L^{-1} Cu^{2+} at 25°C, under continuous magnetic stirring. The amount of the adsorbed Cu^{2+} was determined by measuring the concentration of the Cu^{2+} in the solution. The percentage of Cu^{2+} removal η (%) and adsorption capacity q_e (mg/g) was calculated by Eqs. (1) and (2) as follows:

$$\eta = \frac{(C_0 - C_e)}{C_0} \quad (1)$$

$$q_e = \frac{V(C_0 - C_e)}{m} \quad (2)$$

C_0 and C_e: initial and equilibrated concentrations of Cu^{2+} (mg L^{-1}), respectively; V: the volume of the aqueous solution (L); m: the mass of adsorbent (g).

The concentrations of metal ions were measured through a ternary-complex method, the details are as follows [22]: Cu^{2+}, Rhodamine B, and KI could form negative complex ions, which had the special absorption wavelength around 590 nm. The intensity of absorption peak (located at 592 nm) can be used to represent the concentration of Cu^{2+}. The concentrations of Cu^{2+} were measured by ultraviolet–visible (UV–vis) spectroscope (Lambda 850, PerkinElmer). So a standard curve was firstly drawn by measuring the intensity of the absorption peaks of the negative complex ions with known Cu^{2+} concentrations. And when the absorption peak intensities of the negative complex ions were measured, the concentrations of Cu^{2+} can be calculated through comparison with the corresponding standard curves.

Regarding the isotherm experiments [23], a series of adsorbents with 20, 40, 60, 80, and 100 mg were, respectively, added to 5.0 mg L^{-1} of 50 mL Cu^{2+} solution at pH 4.0 under continuous magnetic stirring and constant reaction time of 90 min throughout the adsorption experiment. The experiments were conducted at different temperatures of 25, 35, and 45°C. Both the Langmuir and the Freundlich models could perform the experimental data conducted.

2.4. Characterization of morphology and structure

The viscosity was measured with a rotational viscometer (NDJ-1, Shanghai Precision and Scientific Instrument Co., China) at 25°C. Electrical conductivity was measured with an electric conductivity meter (G series, CM40G, TOA Electronics, Japan). The diameter and morphology of specimens were observed on SEM (JSM-7500LV, JEOL) Specimens were sputter coated with platinum before SEM observation. The diameter and pore size were measured by the SEM software Smile-view (version 2.0, JEOL). The porosity and specific surface areas were characterized by N_2 adsorption–desorption isotherm analysis (Micromeritics ASAP2020 apparatus at 77 K).

3. Results and discussion

Fig. 1(A) shows SEM of non-porous CA fibrous membranes (FCA) prepared by electrospinning 12 wt.% CA solutions using 1:2 (v/v) DMF/acetone as solvent. Relative smooth and round fibers with diameters of 0.48 ± 0.10 μm were obtained. Liu and Tang [24] reported cellulose acetate fibrous membranes with smooth surface prepared by electrospinning of cellulose acetate in solvent mixture *N, N*-dimethylacetamide (DMAc)/acetone. This result was in agreement with this work. Fig. 1(B) shows SEM of CA membranes (MCA) with a smooth surface prepared by tape casting. A mass of similar behavior was observed in membranes obtained by tape casting.

Non-porous CA fibrous membranes were obtained using 1:2 (v/v) DMF/acetone as solvent. This attributed that the boiling point of DMF/acetone (T_b = 88.3°C) was high. Since solvent evaporation was slow, as the jet arrived before collector, a bigger temperature gradient between the surface of the jet and the bulk was not obtained. Therefore, the non-porous fibers were obtained when the solvent completely volatilized. Based on the above reasons, in order to obtain nanoporous structures CA fibrous membranes, the highly volatile acetone/DCM (T_b = 42.4°C) mixture solvent was used instead of 1:2 (v/v) DMF/acetone. Fig. 2(A) shows the SEM of nanoporous structure CA fibrous membranes (NPCA) with a diameter of 0.94 ± 0.36 μm (Table 1). The viscosity and conductivity of CA-DMF/acetone (1:2) solution were 0.10 Pa s and 10.23 μs/cm and of CA-acetone/DCM (1:4) solution, 0.18 Pa s and 6.30 μs/cm. Therefore, 1:4 (v/v) acetone/DCM mixture solvent yielded thicker CA fibers because of the less stretching of the jet since these solutions have high viscosity and low conductivity values. In addition, ribbon-like fibers are formed (Fig. 2(A,B)) by the collapse of a tube-like fiber skin due to a rapid vaporization of solvent from the inside of the fiber and atmospheric pressure tends to collapse the tube formed by the skin as the solvent evaporated [25]. The SEM images of NPCA with higher magnifications are given in Fig. 2(B). It was observed that the nanoporous structure CA fibers with pore sizes of 52 × 98 nm. The porous structure was due to the rapid evaporation of highly volatile 1:4 (v/v) acetone/DCM mixture solvent and a subsequent rapid solidification of CA polymer chains during the electrospinning process. The fast evaporation of solvent gives rise to local phase separation, and the solvent-rich regions transform into pores during the electrospinning process [26].

The placement of DCM by a solvent with high boiling point such as DMF eliminated the pore

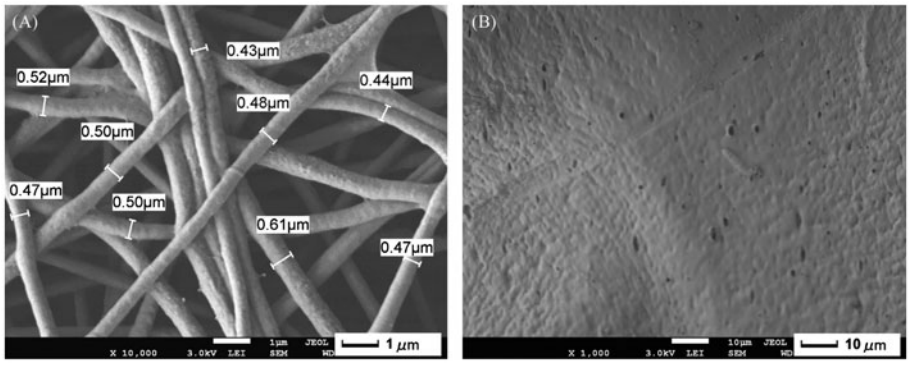

Fig. 1. SEM images of (A) FCA prepared by electrospinning and (B) MCA prepared by tape casting.

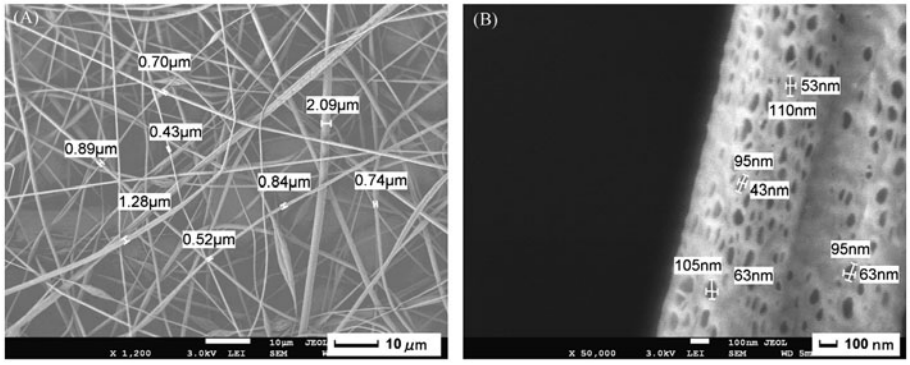

Fig. 2. (A) SEM images of NPCA and (B) Magnification of A.

Table 1
Morphology and BET of the adsorbent

Adsorbent	Morphology	Diameter (μm)	Pore size (nm)	BET (m^2/g)
MCA	Smooth membranes	–	–	0.0029
FCA	Round fibers	0.48 ± 0.10	–	4.33
NPCA	Ribbon-like fibers with nanoporous	0.94 ± 0.36	52 × 98	56.57

formation. When 1:2 (v/v) DMF/acetone solvent system was used, we obtained smooth fibers without the presence of porous structure (Fig. 1(A) and Table 1). In addition, the fibers were round instead of a ribbon-like structure. Therefore, the reason for a porous and ribbon-like structure for CA fibers was because of the highly volatile nature of DCM. The fiber-specific surface area was increased from 4.33 (FCA) to 56.57 m^2/g (NPCA) by the formation of nanoporous structure, which was in favor of the adsorption of Cu^{2+}.

To further understand the pore structure of NPCA, their N_2 adsorption and desorption isotherms were measured. The typical N_2 adsorption–desorption isotherms and pore size distributions of NPCA are shown in Fig. 3. The insets in Fig. 3 are the corresponding pore size distribution (PSD) curves, which were derived by the Barret–Joyner–Halenda (BJH) method. They revealed a pore size distribution centered at about 55 nm. This was in agreement with SEM observation. In addition, the Brunauer–Emmett–Teller (BET) analysis showed that the surface area of the NPCA was 56.57 m^2/g (Table 1).

The adsorption of Cu^{2+} on adsorbent was studied as a function of contact time at 25°C and initial adsorbent concentration of 5.0 mg L^{-1}. As can be seen from Fig. 4, the adsorption of Cu^{2+} on MCA, FCA, and NPCA attained an equilibrium state after 40 min. The adsorption occurred rapidly within the first 10 min,

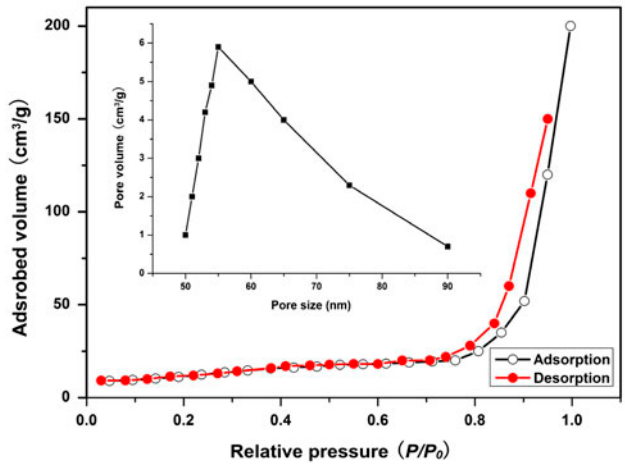

Fig. 3. Nitrogen adsorption and desorption isotherms measured at 77 k for NPCA with the insert showing the pore size distribution curves calculated from the adsorption and desorption branches.

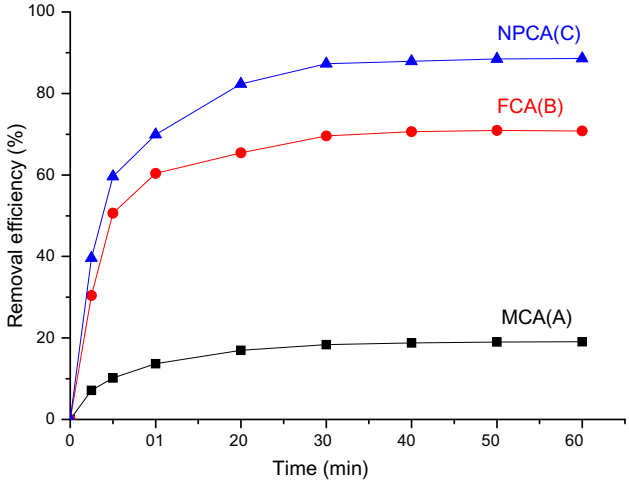

Fig. 4. The removal efficiency of Cu^{2+} from aqueous solutions by different adsorbents: (A) MCA, (B) FCA, and (C) NPCA at 25°C.

which is probably due to the abundant availability of active site, such as hydroxyl group chemically rapidly to combine with Cu^{2+}. The adsorption rate decreased with increasing adsorption time and gradually achieved equilibrium. The maximum removal efficiencies of Cu^{2+} on MCA, FCA, and NPCA were 19.1, 70.8, and 88.6%, respectively. The increase in removal efficiency (NPCA) was certainly attributed to the formation of nanoporous structure on the fibers surface, which increased the special surface area.

Fig. 5 shows the amount of Cu^{2+} adsorbed on NPCA as a function of the equilibrium concentration of Cu^{2+} from aqueous solution. It was shown that the amount of adsorbed Cu^{2+} increased with the increase of the equilibrium concentration at different temperatures. The maximum adsorption capacity of the NPCA was 27.85 mg/g at 318 K. The adsorption data were analyzed by Langmuir and Freundlich models.

The Langmuir isotherm is expressed as follows [27, 28]:

$$\frac{C_e}{q_e} = \frac{1}{q_{\max} b} + \frac{C_e}{q_{\max}} \tag{3}$$

q_e (mg g^{-1}): the equilibrium Cu^{2+} concentration on the adsorbent, C_e (mg L^{-1}): the equilibrium Cu^{2+} concentration in solution, $q_{\max}$ (mg g^{-1}): the maximum adsorption capacity corresponding to complete monolayer adsorption and b (L mg^{-1}): the Langmuir adsorption constant.

The Freundlich isotherm is expressed as follows [29]:

$$\ln q_e = \ln k_f + \frac{1}{n} \ln C_e \tag{4}$$

q_e (mg g^{-1}): the equilibrium Cu^{2+} concentration on the adsorbent, C_e (mg L^{-1}): the equilibrium Cu^{2+} concentration in solution, K_f (L/mg) and n are the Freundlich constants that can be related to the adsorption capacity and the adsorption intensity, respectively.

The experimental data were fitted onto Langmuir and Freundlich models as illustrated in Fig. 6. The values of isotherm constants and correlation coefficients (R^2) are presented in Table 2. The maximum

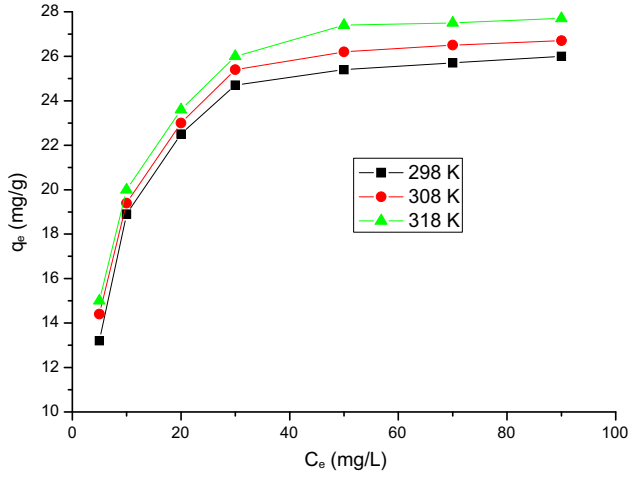

Fig. 5. Adsorption isotherms for Cu^{2+} adsorption by NPCA at different temperatures.

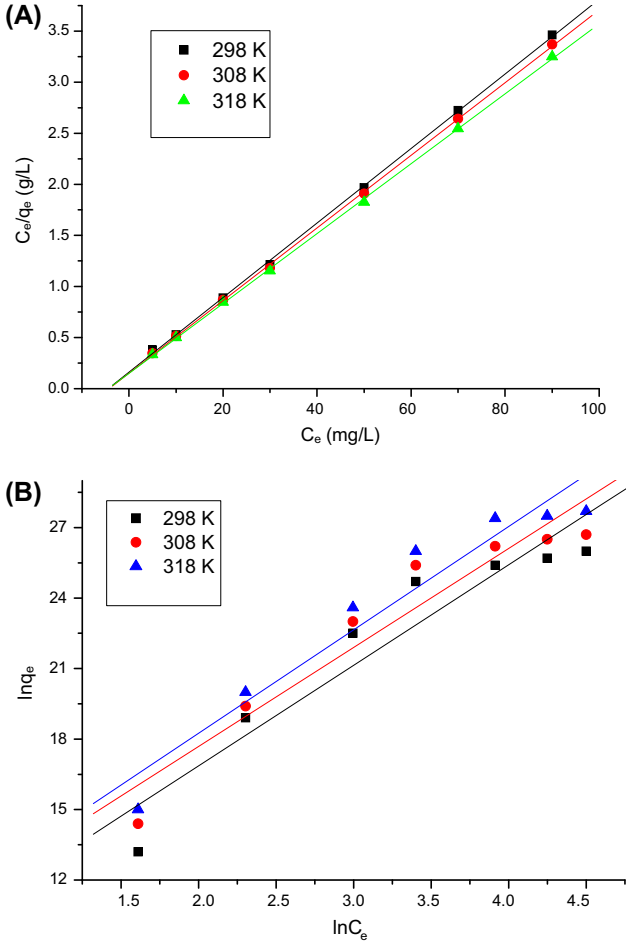

Fig. 6. Linear curve fitted in (A) Langmuir model and (B) Freundlich model for Cu^{2+} adsorption by NPCA.

theoretical adsorption capacity of the NPCA was 28.44 mg/g (318 K) predicted by the Langmuir model, and the estimated values matched well with the experimental value (27.85 mg/g) (Fig. 5). The reference reported that the maximum theoretical adsorption capacities of Cu^{2+} for other adsorbents were in range of 50.45–19.20 (mg/g) [3,30–32]. The result showed that NPCA had a good ability for Cu^{2+} sorption. Moreover, the R^2 was about 0.999 and 0.929 for Langmuir and Freundlich models, respectively, which indicates that the Langmuir model provided the better fit to the experimental data [33].

The thermodynamic parameters of Cu^{2+} adsorption by NPCA, such as the change of Gibbs free energy (ΔG°), the standard enthalpy change (ΔH°), and standard entropy change (ΔS°), could be calculated from the experimental data obtained at different temperatures in the range of 298–338 K. The relationship between ΔG° and K_D is given by the following (5)–(7) equations[34,35]:

$$\Delta G^0 = -RT \ln K_D \tag{5}$$

$$\ln K_D = \frac{\Delta S^0}{R} - \frac{\Delta H^0}{RT} \tag{6}$$

$$K_D = \frac{q_e}{C_e} \tag{7}$$

K_D: the sorption distribution coefficient, T (K): temperature, R (J (mol K)$^{-1}$): the ideal gas constant, q_e (mg g^{-1}): the equilibrium Cu^{2+} concentration on the adsorbent, and C_e (mg L^{-1}): the equilibrium Cu^{2+} concentration in solution.

The plots of lnK_D vs. 10^3/T are shown in Fig. 7. The values of the thermodynamic parameters are collected in Table 3. As can be presented in Table 3, the negative values of ΔG° at all temperatures indicated that the adsorption of Cu^{2+} on PFCA was spontaneous and thermodynamically favorable. Moreover, ΔG° value decrease from −2.560 to −6.701 with the increasing temperature from 298 to 338 K shows that the adsorption reaction for Cu^{2+} on PFCA was more spontaneous at high temperature, indicating that the adsorption processes are favored in high temperature. The positive value of ΔH° (20.337 kJ mol^{-1}) demonstrates that the adsorption process belongs to endothermic nature, revealing that high temperature is more beneficial for adsorption than low temperature. Irani et al. [36] reported that the ΔH° values lie in the ranges of 2.1–20.9 and 80–200 kJ mol^{-1} for physical and chemical adsorptions, respectively. Therefore, the adsorption of Cu^{2+} onto the NPCA belonged to physical adsorption. The ΔS°, equal to 0.121 J mol^{-1} K^{-1},

Table 2
Fitted parameters of Langmuir and Freundlich models

	Langmuir			Freundlich		
T/K	R^2	q_{max}/(mg/g)	b/(L/mg)	R^2	n	K_f (mg/g)
298	0.9994	27.40	0.226	0.9194	3.3	5.6
308	0.9996	28.11	0.237	0.9195	3.5	6.1
318	0.9996	28.44	0.228	0.9326	3.7	6.7

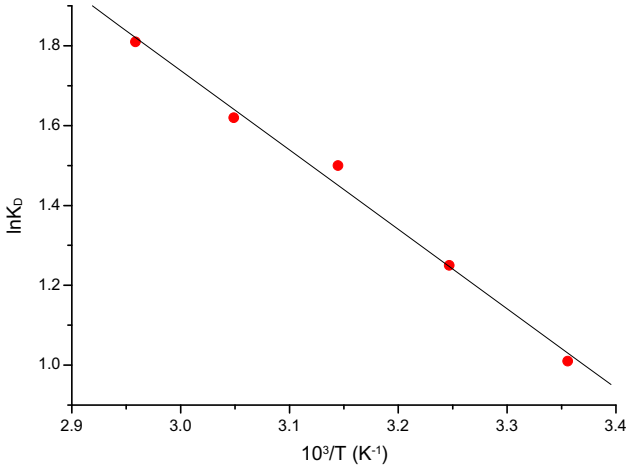

Fig. 7. The relationship between $\ln K_D$ and $10^3/T$ for Cu^{2+} adsorption by NPCA.

Table 3
Thermodynamics parameters for the adsorption of Cu^{2+} on the NPCA

T (K)	ΔG° (kJ mol^{-1})	ΔH° (kJ mol^{-1})	ΔS° (J mol^{-1} K^{-1})
298	−2.560	20.337	0.121
308	−3.544		
318	−4.517		
328	−5.489		
338	−6.701		

indicated the increased randomness at the solid/solution interface with some structural changes in both the adsorbates and adsorbents during the adsorption process.

4. Conclusions

In this study, nanoporous structure CA ultrafine fibers were prepared by electrospinning using 1:4 (v/v) acetone/DCM as solvent used as adsorbent for removing Cu^{2+} from aqueous solutions. The experimental data were fitted into Langmuir and Freundlich models, and Langmuir model provide the better fit to the experimental data. The maximum theoretical adsorption capacities of the NPCA was 28.44 mg/g, which indicated that NPCA had a good ability for Cu^{2+} sorption. Thermodynamic parameters were calculated and the results revealed that the adsorption of Cu^{2+} on NPCA was spontaneous and endothermic. This study had provided the new method to prepare nanoporous structure electrospun fibers, which were used to treat wastewater.

Acknowledgment

This work is supported by the Research Fund for the Doctoral Program of Higher Education of China (No. 20123503110003), the Natural Science Foundation of Guangxi Province (No. 2013GXNSFBA019036), the Natural Science Foundation of Fujian Province (No. 2010J06017), the National Natural Science Foundation of China (No. 51406141), Project of Fujian Province Education Department (JK2012055, JA13320), and the National Undergraduate Innovative Test Program (201210397003).

References

[1] A.K. Meena, G.K. Mishra, P.K. Rai, C. Rajagopal, P.N. Nagar, Removal of heavy metal ions from aqueous solutions using carbon aerogel as an adsorbent, J. Hazard. Mater. 122 (2005) 161–170.
[2] B. Yu, Y. Zhang, A. Shukla, S.S. Shukla, K.L. Dorris, The removal of heavy metal from aqueous solutions by sawdust adsorption—removal of copper, J. Hazard. Mater. 80 (2000) 33–42.
[3] B. Amarasinghe, R.A. Williams, Tea waste as a low cost adsorbent for the removal of Cu and Pb from wastewater, Chem. Eng. J. 132 (2007) 299–309.
[4] L.X. Li, J.H. Dong, T.M. Nenoff, Transport of water and alkali metal ions through MFI zeolite membranes during reverse osmosis, Sep. Purif. Technol. 53 (2007) 42–48.
[5] H.F. Cheng, Cu (II) removal from lithium bromide refrigerant by chemical precipitation and electrocoagulation, Sep. Purif. Technol. 52 (2006) 191–195.
[6] R.P. Han, W.H. Zou, Z.P. Zhang, J. Shi, J.J. Yang, Removal of copper (II) and lead (II) from aqueous solution by manganese oxide coated sand: I. Characterization and kinetic study, J. Hazard. Mater. 137 (2006) 384–395.
[7] C. Blöcher, J. Dorda, V. Mavrov, H. Chmiel, N.K. Lazaridis, K.A. Matis, Hybrid flotation—membrane filtration process for the removal of heavy metal ions from wastewater, Water Res. 37 (2003) 4018–4026.
[8] S. Rengaraj, S.H. Moon, Kinetics of adsorption of Co (II) removal from water and wastewater by ion exchange resins, Water Res. 36 (2002) 1783–1793.
[9] C.Y. Tang, H.Q. Liu, Cellulose nanofiber reinforced poly (vinyl alcohol) composite film with high visible light transmittance, Compos. Part A: Appl. Sci. Manuf. 39 (2008) 1638–1643.
[10] M.M. Bergshoef, G.J. Vancso, Transparent nanocomposites with ultrathin, electrospun nylon-4,6 fiber reinforcement, Adv. Mater. 11 (1999) 1362–1365.
[11] T.P. Cao, Y.J. Li, C.H. Wang, L.M. Wei, C.L. Shao, Y.C. Liu, Fabrication, structure, and enhanced photocatalytic properties of hierarchical CeO_2 nanostructures/TiO_2 nanofibers heterostructures, Mater. Res. Bull. 45 (2011) 1406–1412.
[12] T. Cao, Y. Li, C. Wang, C. Shao, Y. Liu, A facile in situ hydrothermal method to $SrTiO_3$/TiO_2 nanofiber heterostructures with high photocatalytic activity, Langmuir 27 (2011) 2946–2952.

[13] S.H. Wei, M.H. Zhou, W.P. Du, Improved acetone sensing properties of ZnO hollow nanofibers by single capillary electrospinning, Sens. Actuators B: Chem. 160 (2011) 753–759.
[14] C.S. Zhou, Y.L. Shi, X.D. Ding, M. Li, J.J. Luo, Z.Y. Lu, D. Xiao, Development of a fast and sensitive glucose biosensor using iridium complex-doped electrospun optical fibrous membrane, Anal. Chem. 85 (2012) 1171–1176.
[15] S. Haider, S.-Y. Park, Preparation of the electrospun chitosan nanofibers and their applications to the adsorption of Cu (II) and Pb(II) ions from an aqueous solution, J. Memb. Sci. 328 (2009) 90–96.
[16] C.H. Xiang, M.W. Frey, A.G. Taylor, M.E. Rebovich, Selective chemical absorbance in electrospun nonwovens, J. Appl. Polym. Sci. 106 (2007) 2363–2370.
[17] E.D. Boland, G.E. Wnek, D.G. Simpson, K.J. Pawlowski, G.L. Bowlin, Tailoring tissue engineering scaffolds using electrostatic processing techniques: A study of poly (glycolic acid) electrospinning, J. Macromol. Sci. Part A 38 (2001) 1231–1243.
[18] R. Gopal, S. Kaur, C.Y. Feng, C. Chan, S. Ramakrishna, S. Tabe, T. Matsuura, Electrospun nanofibrous polysulfone membranes as pre-filters: Particulate removal, J. Memb. Sci. 289 (2007) 210–219.
[19] L.F. Zhang, T.J. Menkhaus, H. Fong, Fabrication and bioseparation studies of adsorptive membranes/felts made from electrospun cellulose acetate nanofibers, J. Memb. Sci. 319 (2008) 176–184.
[20] C.M. Buchanan, R.M. Gardner, R.J. Komarek, Aerobic biodegradation of cellulose acetate, J. Appl. Polym. Sci. 47 (1993) 1709–1719.
[21] Y. Tian, M. Wu, R.G. Liu, Y.X. Li, D.Q. Wang, J.J. Tan, R.C. Wu, Y. Huang, Electrospun membrane of cellulose acetate for heavy metal ion adsorption in water treatment, Carbohydr. Polym. 83 (2013) 743–748.
[22] Y. Tian, M. Wu, R.G. Liu, Y.X. Li, D.Q. Wang, J.J. Tan, R.C. Wu, Y. Huang, Electrospun membrane of cellulose acetate for heavy metal ion adsorption in water treatment, Carbohydr. Polym. 83 (2011) 743–748.
[23] W.B. Wang, Y.R. Kang, A.Q. Wang, One-step fabrication in aqueous solution of a granular alginate-based hydrogel for fast and efficient removal of heavy metal ions, J. Polym. Res. 20 (2013) 101–110.
[24] H.Q. Liu, C.Y. Tang, Electrospinning of cellulose acetate in solvent mixture N,N-dimethylacetamide (DMAc)/acetone, Polym. J. 39 (2007) 65–72.
[25] S. Koombhongse, W.X. Liu, D.H. Reneker, Flat polymer ribbons and other shapes by electrospinning, J. Polym. Sci., Part B: Polym. Phys. 39 (2001) 2598–2606.
[26] A. Celebioglu, T. Uyar, Electrospun porous cellulose acetate fibers from volatile solvent mixture, Mater. Lett. 65 (2011) 2291–2294.
[27] G. Alagumuthu, M. Rajan, Equilibrium and kinetics of adsorption of fluoride onto zirconium impregnated cashew nut shell carbon, Chem. Eng. J. 158 (2010) 451–457.
[28] N. Viswanathan, S. Meenakshi, Enhanced fluoride sorption using La(III) incorporated carboxylated chitosan beads, J. Colloid Interface Sci. 322 (2008) 375–383.
[29] D.L. Liu, D.Z. Sun, Y.Q. Li, Removal of Cu (II) and Cd (II) from aqueous solutions by polyaniline on sawdust, Sep. Sci. Technol. 46 (2010) 321–329.
[30] D. Zhou, L.N. Zhang, J.P. Zhou, S.L. Guo, Cellulose/chitin beads for adsorption of heavy metals in aqueous solution, Water Res. 38 (2004) 2643–2650.
[31] K.S. Hui, C.Y.H. Chao, S.C. Kot, Removal of mixed heavy metal ions in wastewater by zeolite 4A and residual products from recycled coal fly ash, J. Hazard. Mater. 127 (2005) 89–101.
[32] J.W. Lin, Y.H. Zhan, Z.L. Zhu, Adsorption characteristics of copper (II) ions from aqueous solution onto humic acid-immobilized surfactant-modified zeolite, Colloids Surf. A: Physicochem. Eng. Aspects 384 (2011) 9–16.
[33] S. Meenakshi, N. Viswanathan, Identification of selective ion-exchange resin for fluoride sorption, J. Colloid Interface Sci. 308 (2007) 438–450.
[34] G. Yan, T. Viraraghavan, Heavy metal removal in a biosorption column by immobilized M. rouxii biomass, Bioresource Technol. 78 (2001) 243–249.
[35] C.K. Na, H.J. Park, Defluoridation from aqueous solution by lanthanum hydroxide, J. Hazard. Mater. 183 (2010) 512–520.
[36] M. Irani, A.R. Keshtkar, M.A. Mousavian, Removal of Cd (II) and Ni (II) from aqueous solution by PVA/TEOS/TMPTMS hybrid membrane, Chem. Eng. J. 175 (2011) 251–259.